Pertanika J. Sci. & Technol. 31 (6): 2735 - 2750 (2023)

PERTANIKA JOURNALS

SCIENCE & TECHNOLOGY

Journal homepage: http://www.pertanika.upm.edu.my/

Effect of Scaling the Electrostatic Interactions on the Free Energy of Transfer of Azurin from Water to Lipid Membrane Determined by Coarse-grained Simulations

Dian Fitrasari[1], Acep Purqon[1] and Suprijadi[1,2]*

[1]Department of Physics, Bandung Institute of Technology, Bandung, Jawa Barat 40132, Indonesia
[2]Research Centre of Nanoscience and Nanotechnology, Bandung Institute of Technology, Bandung, Jawa Barat 40132, Indonesia

ABSTRACT

Azurin protein potentially plays an important role as an anti-cancer therapeutic agent, particularly in treating breast cancer in experiments and showing without having a negative effect on normal cells. Although the interaction mechanism between protein and lipid membrane is complicated, it can be modeled as protein-lipid interaction. Since the all-atom (AA) model simulation is cost computing, we apply a coarse-grained (CG-MARTINI) model to calculate the protein-lipid interaction. We investigate the binding free energy value dependency by varying the windows separation and electrostatic scale parameters. After scaling the electrostatic interactions by a factor of 0.04, the best result in terms of free energy is -140.831 kcal/mol, while after window-separation optimization, it reaches -71.859 kcal/mol. This scaling was necessary because the structures from the CG MARTINI model have a higher density than the corresponding all-atom structures. We thus postulate that electrostatic interactions should be scaled down in this case of CG-MARTINI simulations.

Keywords: Coarse-Grained MARTINI method, electrostatic scaling, free energy analysis, protein-lipid membrane model, windows separation

ARTICLE INFO

Article history:
Received: 20 September 2022
Accepted: 06 March 2023
Published: 08 September 2023

DOI: https://doi.org/10.47836/pjst.31.6.06

E-mail addresses:
dianfitrasari30@gmail.com (Dian Fitrasari)
acep.purqon@itb.ac.id (Acep Purqon)
suprijadi@itb.ac.id (Suprijadi)
* Corresponding author

INTRODUCTION

Azurin is one of the blue copper proteins known as an anti-cancer agent (Frauenfelder et al., 2009), and it is produced by the gram-negative bacteria *Pseudomonas aeruginosa*. Azurin is widely known as a donor in the electron transfer process (Pozdnyakova & Wittung-Stafshede, 2001). Moreover, the

ISSN: 0128-7680
e-ISSN: 2231-8526

blue copper ions in the Azurin active site contribute to this protein's stability (Pozdnyakova & Wittung-Stafshede, 2001; Pozdnyakova et al., 2002). Furthermore, the protein is also an anti-cancer agent that causes apoptosis without much negative effect in cancer patients when it enters the human breast cancer cells (Frauenfelder et al., 2009). The less negative effect in Azurin interaction relates to the interaction with the normal cell under treatment. It represents the relation between Azurin as the protein and membrane lipids. The interaction between protein and membrane accommodates such essential processes, i.e., membrane trafficking, membrane protrusions, cytokinesis, signaling, and cell communication (Arumugam et al., 2011).

The interaction between protein and membrane has been modelized by membrane insertion. The challenge of this model is to identify the folded structure of the protein membrane. The sequence statistic succeeded in the comprehensive understanding of energy, which enforces the importance of membrane insertion to acknowledge this challenge. Numerous work approach has been made to define the free energy of amino-acid insertion. There are disagreements between experiment and theory. On the other hand, molecular dynamic simulation has been developed through various applications of membrane insertion and reproducing experimental free energy. However, the differences in microscopic processes make usable free energy of membrane insertion difficult (Gumbart & Roux, 2012).

Free energy transfer has been determined for arginine and leucine amino acids using Free Energy Perturbation (FEP) method. There is a significant result regarding the insertion penalty. The result is reduced and has the same compression observed in the experiment-based scale (Gumbart et al., 2011). On the other hand, simulation time challenges and precision dynamics to study the fluctuation of this interaction establish researchers to develop various models and methods. One type of model which narrates the complex simulation with efficient time is the CG-MARTINI model by Marrink et al. (2007).

The CG models typically provide the mapping of four heavy atoms of Carbon (C), Nitrogen (N), Oxygen (O), and Phosphor (P) in one bead. The mapping definition builds the complex system, such as protein-lipid interaction, which is less computationally than the AA model. There are some coarse-grained (CG) models, and CG-MARTINI models provide a good model of the protein-lipid environment. However, calculating the precise models from CG-MARTINI is quite challenging because of the different degrees of freedom from the beads mapping.

Since current CG-MARTINI lacks copper information, we use the active site binding from other work's definition (Kurniawan et al., 2019). The copper also describes the electron transfer related to this protein's stabilization. Then, we analyze the dynamics, interaction, and free energy values to understand whether Azurin is favorable in the lipid system. Meanwhile, even with a CG model, free energy calculation still needs a longer

simulation to reach the expected values. This study uses FEP as one widely known method to calculate precise energy values. In general, the FEP application is used for calculating small molecules or mutations. The challenge of a complex system with FEP analysis relates to the magnification of perturbation.

For this reason, we optimize the two parameters we expect to impact to reach a shorter simulation and accurate result. The electrostatic scaling parameter was previously studied by Jiang et al. (2009), increasing the acceptance ratio and decreasing free energy values (Li & Nam, 2020). The second parameter which we optimize is an electrostatic scaling parameter. Previous research by Beveridge and DiCapua (1989) also states that the precision of the electrostatic scaling parameter is higher than the Van Der Waals (VDW) parameter.

This work investigates the relation between area per lipid (APL) and density of the CG-MARTINI model with free energy value. To investigate the relationship or scaling between electrostatic parameters and free energy value. We investigate the possibility of finding a scaling factor between CG and all-atom (AA) simulation. The potential candidate parameter could be in tuning the electrostatic parameter so that the electrostatic scaling dependency is interesting to be discussed.

METHODOLOGY

Coarse-grained Method

In this study, the CG-MARTINI model is used to build the protein and membrane lipid structure, and it is a CG model type describing four heavy atoms in one bead. The definition of beads makes the complex system simulation achievable with less computational cost. Although the CG-MARTINI has less resolution and diverges from the AA model, the physical properties can maintain for the whole system. This model widely uses in a complex system to understand the dynamic trend.

Free Energy Perturbation (FEP)

Alchemical FEP can analyze the physical properties in this research. In this method, the Hamiltonian system is defined by the general extent parameter, λ, and the initial state, a, and the final state, b, can be connected by this parameter. It is described and achieved by the Hamiltonian linear combination by Beveridge and Mark (Beveridge & DiCapua, 1989; Mark, 1998). Equation 1 is as follows:

$$H(x, p_x;\ \lambda) = H_0(x, p_x) + \lambda H_b(x, p_x) + (1 - \lambda) H_a(x, p_x) \quad (1)$$

$H_a(x, p_x)$ describes the Hamiltonian for the group of atoms, representing the initial state a. Meanwhile, $\lambda H_b(x, p_x)$ is the interaction of the final state, b. Hamiltonian $H_0(x, p_x)$ describes atoms that are not transforming during simulation. Furthermore, λ and $1 - \lambda$

are the initial and final Hamiltonian parameters. Those parameters describe the function of energy and forces.

In this equation, the coupling parameter is shown as λ_{LJ}. It is a scale of the Lennard-Jones interactions. Electrostatic interactions describe as λ_{elec}. The actual value of λ is as stated in Equation 2:

$$V_{NB}(r_{ij}) = \lambda_{LJ}\epsilon_{ij}\left[\left(\frac{R_{ij}^{min\,2}}{r_{ij}^2+\delta(1-\lambda_{LJ})}\right)^6 - \left(\frac{R_{ij}^{min\,2}}{r_{ij}^2+\delta(1-\lambda_{LJ})}\right)^3\right] + \lambda_{elec}\frac{q_i q_j}{\epsilon_1 r_{ij}} \quad (2)$$

The free energy calculation will not change the intermolecular bonded potentials in this method. The perturbed atom which interacts in a vacuum is scale. However, in hydration conditions, the interaction is scale is only non-bonded interactions. The free energy difference, which is defined between the initial and final state, is as stated in Equation 3:

$$\Delta A_{a\to b} = -\frac{1}{\beta}\ln\langle\exp\{-\beta[H_b(x,p_x) - H_a(x,p_x)]\}\rangle \quad (3)$$

Here, $\beta^{-1} \equiv k_B T$. The Boltzmann constant and temperature describe by k_B and T, respectively. The Hamiltonian for states a and b describes by $H_a(x,p_x)$ and $\lambda H_b(x,p_x)$, respectively. The ensemble average over configuration denotes by $\langle\cdots\rangle_a$. It is representative of the initial reference state, a. The a series of transformations between non-physical, intermediate states along a well-delineated pathway that connects a to b is replacing the transformation between two thermodynamic states. Here we assume the Helmholtz free energy (A) is under the constant volume. Meanwhile, the constant-pressure system thermodynamics should be described by Gibbs free energy (G), with $G=A+PV$, where P is pressure, and V is volume. However, the PV term is typically small for biomolecule systems (Zhu et al., 2022). In conclusion, we consider the $\Delta A_{a\to b} = \Delta G_{a\to b}$.

The pathway is characterized by the general extent parameter λ, causing the Hamiltonian and the free energy as a continuous function between a and b (Equation 4):

$$\Delta G_{a\to b} = -\frac{1}{\beta}\ln\langle\exp\{-\beta[H(x,p_x;\lambda_{i+1}) - H(x,p_x;\lambda_i)]\}\rangle \quad (4)$$

N describes the number of intermediate stages. Meanwhile, Gibbs's free energy, which we use in this work, is absolute free energy symbolized by ΔG.

Model and Software Package

We perform the molecular dynamic simulation in this study using the NAMD 2.12-multicore program package (Phillips et al., 2020). Visualizing Azurin and lipid membrane use VMD 1.9.3 (Humphrey et al., 1996). The initial configuration of Azurin obtains from a protein data bank with PDB ID: 1AZU (Adman & Jensen, 1981), while The VMD 1.9.3 is used to

prepare the initial structure coordinates for the MARTINI CG model through the coarse-grained builder menu. Moreover, the Azurin structure has 128 residues and comprises two layers of sheet-β with eight β-strands. This initial state uses a 2.7 Å resolution X-ray structure. The initial configuration of Azurin contains 930 atoms with one copper.

The AA structure is then modeled in CG structure. This process maps 930 atoms to 269 beads. The hydration state is defined by adding water molecules in the form of BP_4 (Marrink et al., 2007) to prevent the water from freezing at room temperature. This anti-freeze (AF) water model contains around 10% of total water molecules. The salt concentration of this model is 0.1 mol/L, and the coulomb potential defines by cut-offs 9 Å and 15 Å. The minimization and equilibration time step is 10 fs with an NPT ensemble. The final state contains the water molecules and POPC lipid membrane and is neutralized by adding 3 Na^+ ions. In this state, the molecules of POPC are assigned as atoms that appear during the simulation. The parameter that shows atoms appearing during a simulation is flag characterization. The flag characterization is shown as a +1.00 value if the atoms appear in the final state. This model represents a system with a salt concentration of 0.1 mol/L.

RESULTS AND DISCUSSION

In this study, we have two models of Azurin. The first model describes Azurin hydration, and the second describes Azurin with POPC membrane lipids. In the first model, we analyze free energy hydration. We analyze free energy values in the second model by optimizing the separation of the windows ($\delta\lambda$) and electrostatic parameters λ_{elec} using various parameters.

Azurin Hydration

The first model describes the free energy of hydration Azurin. In this model, we define two states, the Azurin appearing in the final state by flag characterization +1.00. The environment described by the water molecule remains still, defined by 0.00 flag characterization. The free energy value is defined by the change of exnihilated to annihilation Azurin in water. The scheme of the perturbation by this system is shown in Figure 1.

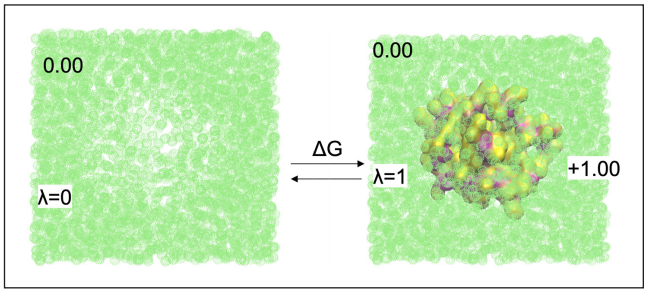

Figure 1. Scheme for free energy calculation in the model I, λ=0 represents the water system as the initial state, and λ=1 represents the Azurin in water as the final state. The Azurin is shown in the purple and yellow surfaces. The water is shown in the green box. The flag characterization for the water box is 0.00, which means water is unchanged during the simulation. The Azurin system uses flag characterization +1.00, which means appearing in the final state.

The free energy values of Azurin hydration relate to the λ state condition, shown in Figure 1. Figure 2(a) shows the free

energy values as a function of the λ state, and Figure 2(b) shows the average electrostatic energy difference. The dotted line in Figure 2(a) shows the annihilated Azurin free energy. The dotted line in Figure 2(b) shows the annihilated Azurin. The simulation was done for 100000 steps with an electrostatic parameter λ_{elec} = 0.5, Lennard-jones parameter λ_{LJ} = 1.0, and 21($\delta\lambda$ = 0.05) windows separation. The change of free energy hydration is –174.636 kcal/mol. Meanwhile, the average electrostatic energy difference changes are –101.298 kcal/mol.

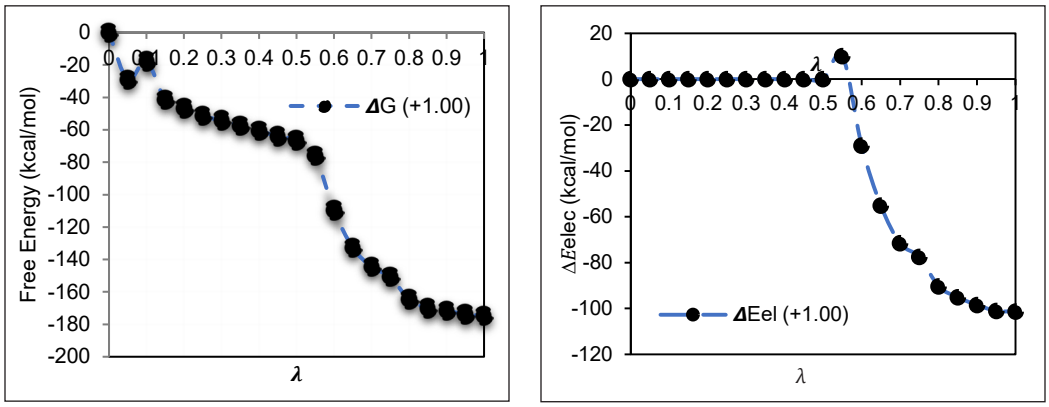

(a) (b)

Figure 2. The analysis of free energy and average electrostatic energy difference in model I: (a) The free energy of annihilated Azurin during simulation with ΔG = –174.636 kcal/mol; and (b) The average electrostatic energy difference of annihilated Azurin: ΔEel = –101.298 kcal/mol.

The Effect of Azurin Insertion in Membrane Lipids POPC

The second model describes the free energy of Azurin in POPC. In this model, we define two states, the Azurin appearing in the final state by flag characterization +1.00. The environment described by the POPC-water remains still, defined by 0.00 flag characterization. It appears Azurin defines the free energy value in POPC. The scheme of the perturbation by this system is shown in Figure 3.

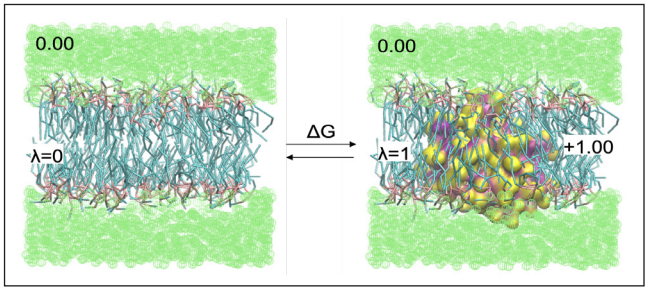

Figure 3. Scheme for free energy calculation in model II. λ=0 represent the POPC system as the initial state, and λ=1 represents the Azurin in POPC as the final state. The Azurin is shown in purple and yellow surface, and the water box is shown in the green box. Moreover, the POPC membrane is shown by lines blue and pink. The flag characterization for the water box is 0.00, which means water is unchanged during the simulation. The Azurin system uses flag characterization +1.0,0, which means appearing in the final state.

The free energy values of Azurin in POPC relate to the state condition, shown in Figure 4. Figure 4(a) shows the free energy values as a function of the λ state, and Figure 4(b) shows the average electrostatic

energy difference. The dotted line in Figure 4(a) shows the annihilated Azurin free energy. The dotted line in Figure 4(b) shows the annihilated Azurin and the straight line shows the changes in average electrostatic energy differences. The simulation was done for 100000 steps with electrostatic parameter $\lambda_{elec} = 0.5$, Lennard-jones parameter $\lambda_{LJ} = 1.0$ and 21($\delta\lambda = 0.05$) windows separation. The changes in free energy hydration are –200.340 kcal/mol. Meanwhile, the average electrostatic energy difference changes are –130.02 kcal/mol.

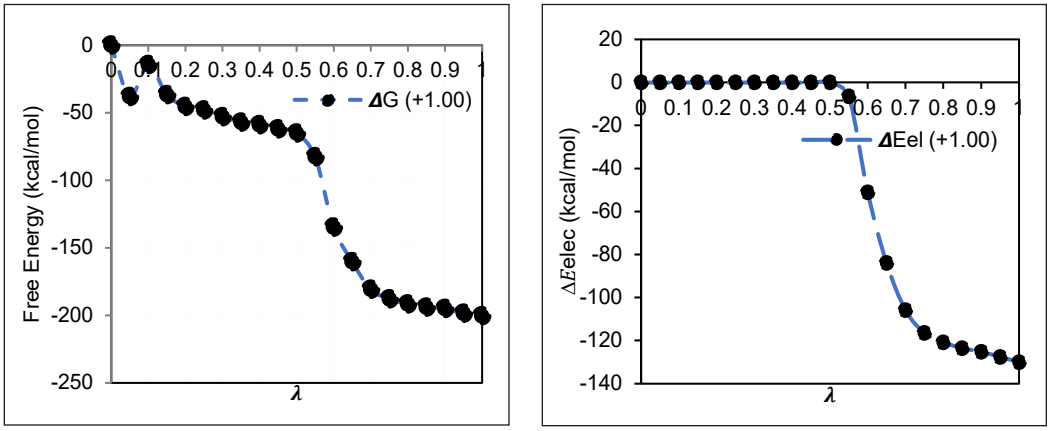

(a) (b)

Figure 4. The analysis of free energy and average electrostatic energy difference in model II. (a) The free energy of annihilated Azurin during simulation with ΔG = –200.340 kcal/mol; (b) The average electrostatic energy difference of annihilated Azurin: ΔEel = –130.02 kcal/mol

The Difference Between Azurin Hydration Free Energy and Azurin Insertion in Membrane Lipids

Figure 5(a) shows the free energy difference between Azurin in water and the POPC lipid membrane. Figure 5(a) shows a dotted line showing Azurin hydration, and the bold line shows Azurin in POPC. Figure 5(b) shows the changes in the average electrostatic energy difference between Azurin hydration and Azurin in POPC. The dotted line shows Azurin hydration, and the bold line shows Azurin on POPC. Both figures show in the POPC lipid membrane that the free energy and electrostatic energy tend to decrease, as shown by the more negative energy. We compare the free energy of Azurin in a different state, shown in Table 1. This table shows that even in the POPC environment, the free energy tends to be more negative. Still, the experimental value shows a larger value indicating some difference in perturbation type for the CG-MARTINI model. However, we can reach efficient ways in terms of simulation time. The effective ways to find the exact value in CG-MARTINI seem related to the non-bonded interaction described in the next part.

The free energy value shows tendencies to make Azurin have like-able tendencies inside the POPC membrane. It is also shown in Table 1, which indicates that Azurin is more favorable in the POPC environment, shown by more negative free energy values.

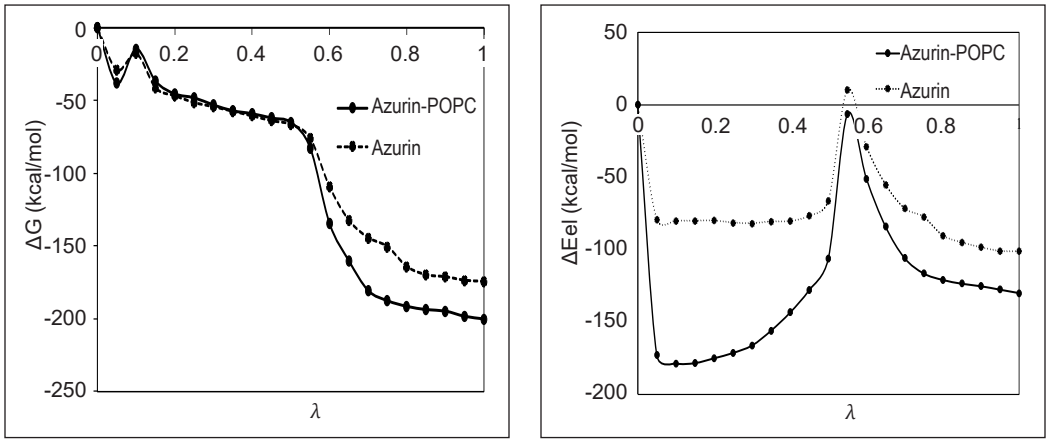

(a) (b)

Figure 5. The analysis of free energy and average electrostatic energy difference for Azurin hydration and Azurin-POPC system. (a) The free energy of annihilated Azurin during simulation with, Azurin-POPC: ΔG = –200.34 kcal/mol, Azurin: ΔG = –174.636 kcal/mol; (b) The average electrostatic energy difference of annihilated Azurin, in POPC:ΔEel = –130.021 kcal/mol, water: ΔEel = –101.298 kcal/mol.

Table 1
The differences in free energy analysis of Azurin in water and POPC, respectively

The System of Azurin	ΔG Experiment Hydration (Pappalardo et al., 2003)	ΔG (Azurin)	ΔG (Azurin-POPC)
Free Energy (kcal/mol)	-32.7438	-174.636	-200.340

The Windows Separation Changes

Table 2 shows the difference in free energy values related to the changes in the windows separation number. In Figure 6(a), we can see that the fewer separation windows value decreases the free energy value. Figure 6(b) also shows the same trend, which changes average electrostatic energy differences. In previous research by Li and Nam (2020), this separation tends to decrease the free energy values in thermodynamic integration (TI) methods. We choose windows separation randomly.

The free energy values tend to increase with window separation addition. The higher acceptance ratio relates to increasing the number of windows, although its cost is computational (Jiang et al., 2009). The separation windows describe the replica of the system.

The free energy relation with windows separation is shown in Figure 7. Figure 7(a) specifically shows the relation between free energy values and the change of windows separation, and Figure 7(b) is about the average electrostatic difference. Although it has polynomial fourth-order tendencies, some average electrostatic difference value looks to decrease in higher separation windows. It also means the trendline is nonlinear between the separation windows and energy changes.

Table 2
The absolute binding free energy (ΔG) of Azurin in POPC membrane (λ_{elec} = 0.5, λ_{LJ} = 1.0, numsteps=100000 steps) with windows (δλ) variations

N(δλ)	3	5	9	11	13	15	17	21	31	41	45	47	48	51	60
Δ*G* (kcal/mol)			-INF		-337.779	-286.619	-252.335	-200.340	-132.227	-104.211	-85.450	-91.329	-87.566	-84.201	-71.859
Δ*Eel* (kcal/mol)					-219.110	-186.900	-163.480	-130.020	-83.616	-68.930	-53.580	-59.49	-57.51	-55.80	-47.827

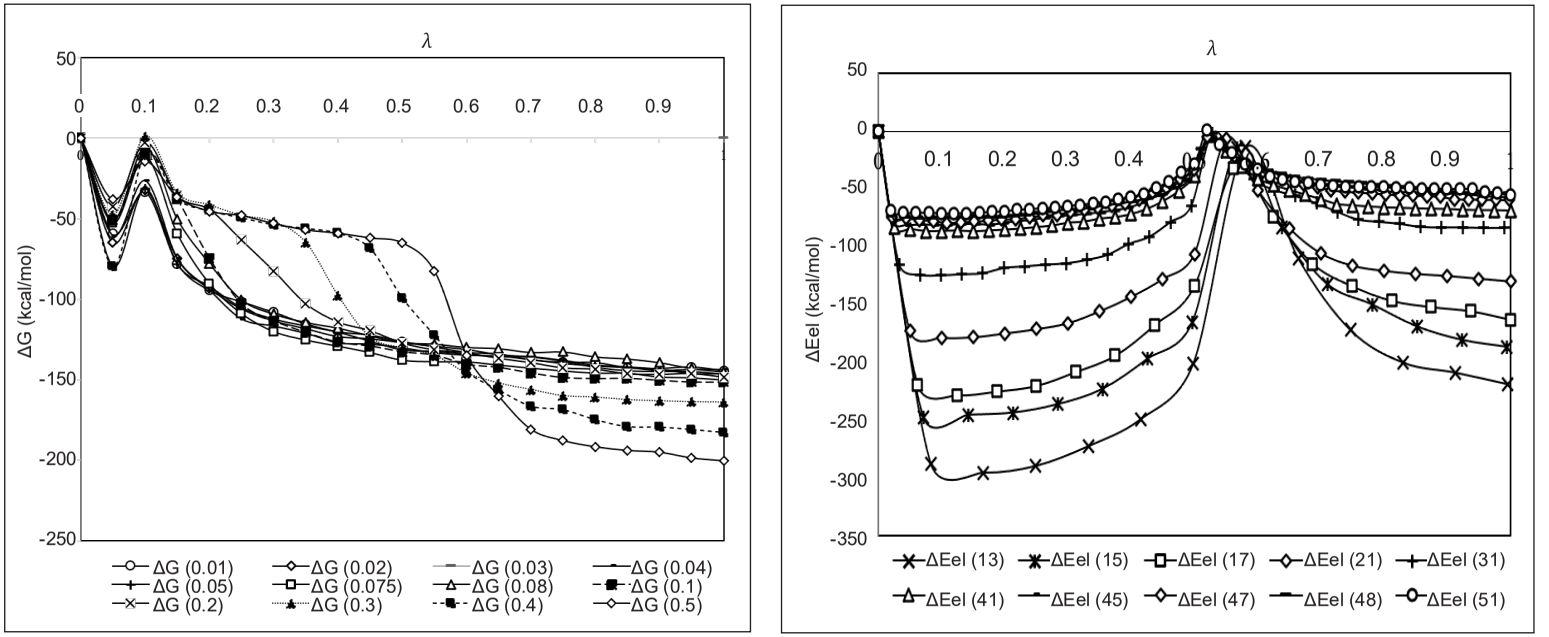

(a) (b)

Figure 6. The analysis of free energy and average electrostatic difference with various windows separation. (a) The relation of free energy and lambda state; (b) The relation of the average electrostatic difference and lambda state

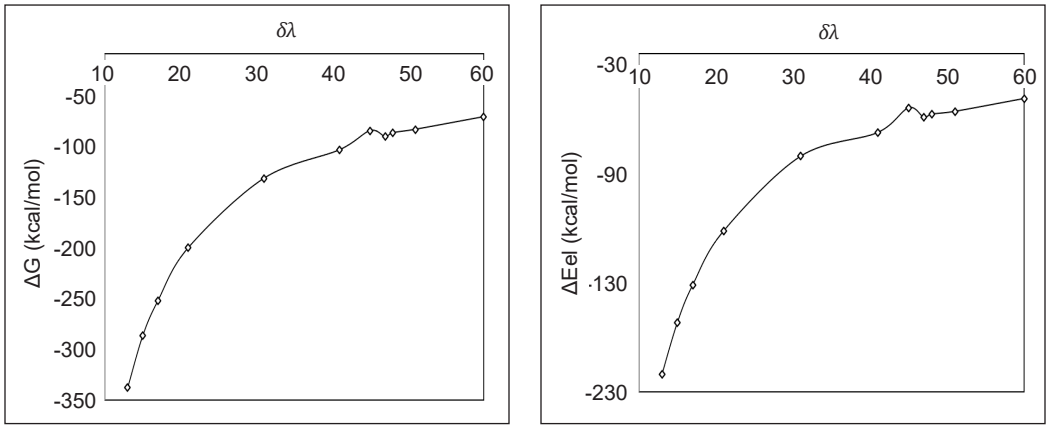

(a) (b)

Figure 7. The relation between free energy, average electrostatic difference, and windows separation. (a) The analysis of free energy and windows separation; (b) The analysis of average electrostatic difference and windows separation

The Electrostatic Parameter Changes

The electrostatic scale parameter affects the changes in the free energy of Azurin shown in Table 3. To find the effect of the electrostatic scale parameter, we introduce the value and relation of this parameter with interatomic distance. In NAMD, which uses free energy perturbation, λ_{elec} A value less than or equal to the user-defined (=0.5).

In FEP calculated by NAMD, the electrostatic parameter is used to avoid "end-point catastrophe," which avoids growing particles overlapping with existing particles with an unbounded interaction potential that will approach infinity as the interaction distance approaches zero.

We can see the additional effect of λ_{elec}. It tends to decrease the free energy values. In this part, we calculate the effect of this parameter in Azurin-POPC systems. We find the free energy differences shown in Table 3.

Table 3
The absolute binding free energy and average electrostatic analysis differentiate by electrostatic parameter values (λ_{LJ} = 10, numstep=100000, δλ=0.05)

λ_{elec}	0.04	0.05	0.075	0.08	0.1	0.2	0.3	0.4	0.5
ΔG (kcal/mol)	-143.859	-146.367	-150.173	-145.040	-151.485	-148.474	-163.879	-182.797	-200.340
ΔEel (kcal/mol)	-81.34	-78.16	-79.92	-76.98	-85.21	-80.21	-95.67	-114.49	-130.02

Figure 8(a) shows the free energy differences related to the electrostatic parameter changes. This figure shows difference curvature, which describes how the energy change when the electrostatic parameter change. It has a higher value in 0.5 values of the electrostatic parameter. Meanwhile, we can assume that lowering this value can get the free energy as expected. Figure 8(b) shows free energy and interatomic distance. We can see that as the free energy reach λ_{elec} = 0.1, the free energy has been saturated, which means the scaling makes the maximal interaction. The free energy tends to saturate after λ_{elec} = 0.1 until the λ_{elec} reaches 0.04. We can see in Figure 8(b) that the curve changes slightly as the interatomic distance becomes larger. We suppose this situation could be because the atom's interaction has reached the peak of interaction.

Figure 9 shows the differences of average electrostatic differences from different electrostatic parameters. The free energy value tends to increase in the lower electrostatic parameter and fade away at the 0.01 value of the electrostatic parameter. We assume this relates to the model which we use. Figure 9(b) shows the average electrostatic difference with interatomic distance. This relation is quite the same with free energy, as we mentioned in Figure 9(b); however, after λ_{elec} = 0.1, it also has some tendencies with free energy values, which have slightly different values.

In CG-MARTINI, the densities become higher than AA, which we can assume may be why there are different free energy values when the electrostatic parameter varies. In a higher electrostatic parameter value, the free energy considers higher, which tends to be close to the Azurin hydration experimental value. We assume the difference in density of the AA model and CG-MARTINI model makes this free energy differs. Table 4 shows the APL from the experiment and our result. It shows that CG-MARTINI has a larger APL.

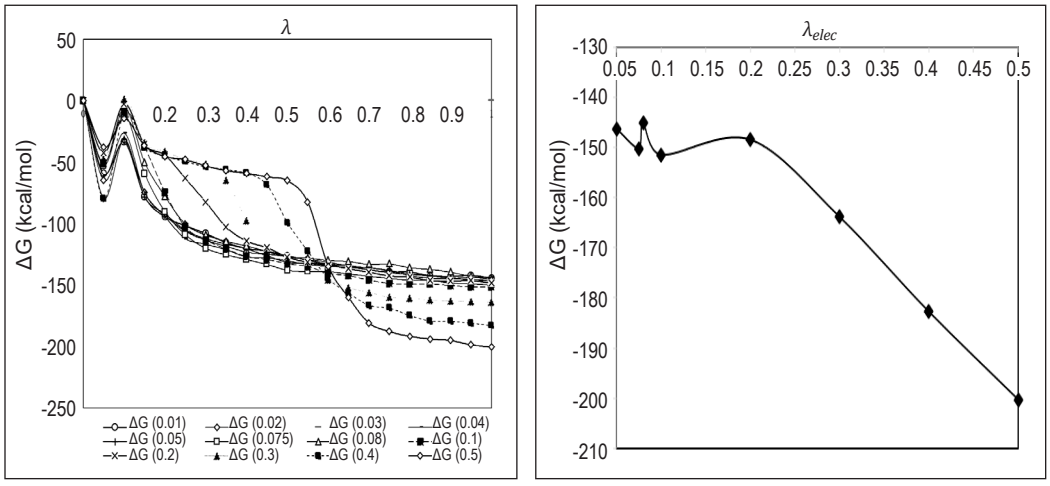

Figure 8. The free energy analysis relates to different electrostatic parameter values. (a) Free energy as a function of λ state; (b) Free energy as a function of the electrostatic scale parameter

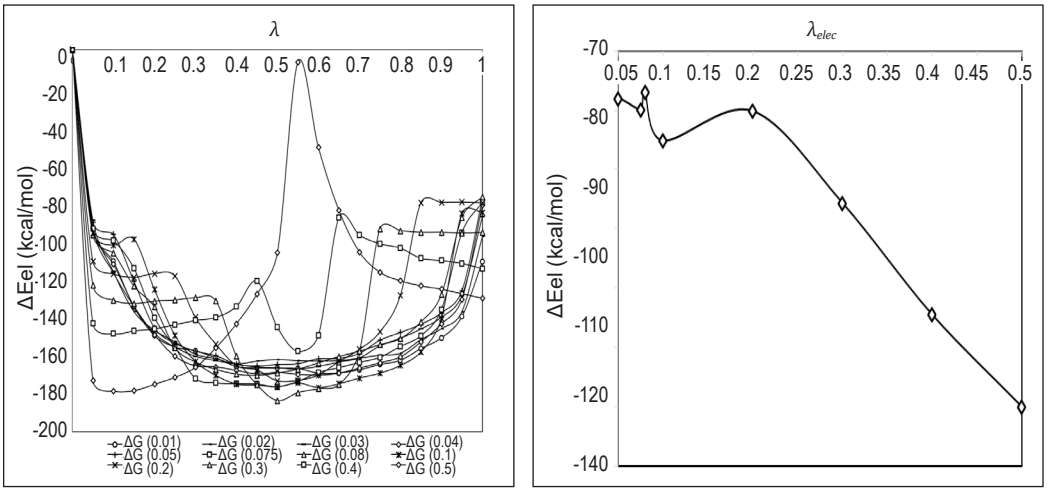

(a) (b)

Figure 9. The average electrostatic difference analysis relates to different electrostatic parameter values. (a) Average electrostatic difference as a function of λ state; (b) Average electrostatic difference as the function of the electrostatic scale parameter

Table 4
The area per lipid (APL) of CG-MARTINI compared to the experiment

	Experiment (Kucerka et al., 2006)	Our result
Area Per Lipid (Å²)	68.3 at 303.15 K	89.4 at 310 K

The CG-MARTINI has a difference in resolution, which impacts density in the same APL. That also explains that this model creates a value gap for free energy. The AA model is closer to free energy in the experiment. However, CG has advantages in terms of cost computing to look for trends, not accuracy. Because of this reason, it might be possible to approach the experiment by varying some of the scaling parameters as the candidates, as we mentioned before.

We illustrate the density change in Figure 10 to understand the magnification of the electrostatic scale parameter in the CG-MARTINI model. From this figure, there are different densities between these two models. Figure 10 shows the AA model mapping to the CG-MARTINI model and the density differences. The changes in the electrostatic scale parameter lead to a different approach through free energy calculation. This work assumes that electrostatic scaling influences the free energy calculation. Since the density in the CG-MARTINI model is larger than an AA model, the rescaling on electrostatic needs to reach the free energy accurately. Based on Beveridge and Dicapua's (1989) work, the change of electrostatic parameters is more precise than van der Waals's parameters related to free energy values. Previous research has shown that the energy and forces dominate by previous interaction before the latter repulsive component becomes larger to prevent

counterfeit collisions from atoms of a constituent during the scaling of Coulomb and Van Der Waals interaction (Pohorille et al., 2010).

The electrostatic scaling is the constant that affects the non-bonded potential related to the distance among atom units. The distance among atoms changes in the CG-MARTINI model, which makes the mass density larger.

The electrostatic scaling in FEP shows how it changes the interatomic distance. However, as shown in Figure 11, we can see that the density values of CG-MARTINI are larger than the AA model by Gurtovenko and Anwar (2009). It explains why the free energy values can change each time the electrostatic parameter has been rescaled. We assume the larger density in CG-MARTINI needs the scaling with a value of 0.05-0.2 because the atoms are tightly bound to one another, which needs some spacing value to make the free energy as expected.

The density of CG-MARTINI is higher than all-atom, so it needs scaling of electrostatic scale parameter to reach the free energy values as expected. Figure 11 shows the density

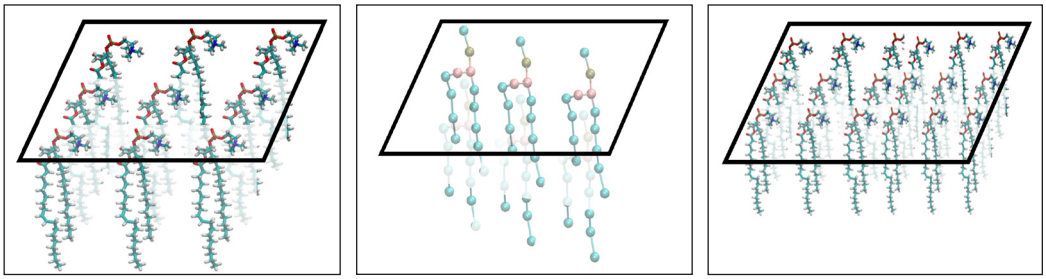

Figure 10. The comparison of CG-MARTINI Model with All-Atom Model: (a) AA Model; (b) CG-MARTINI Model; and (c) CG-MARTINI Model comparison in AA Model

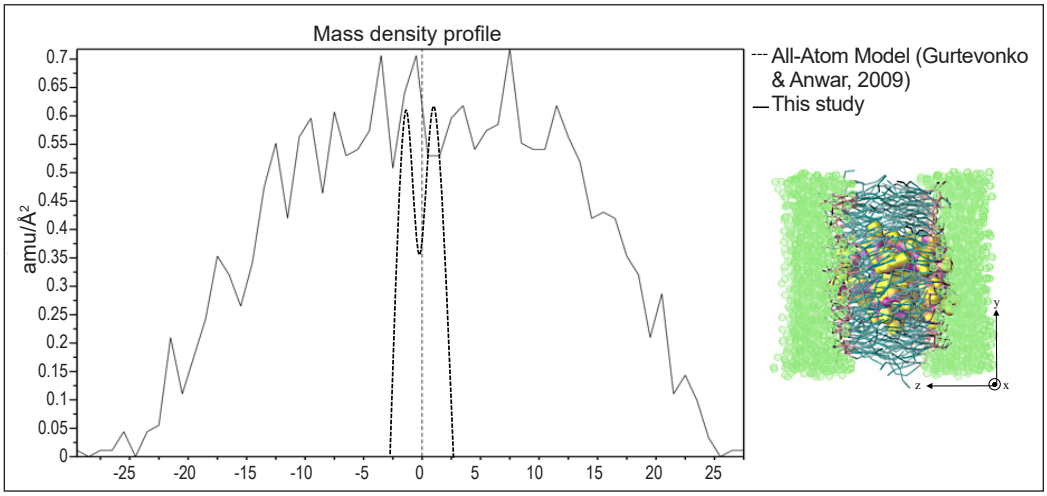

Figure 11. The mass density profile of the CG-MARTINI model compared to the All-Atom Model

change for CG-MARTINI compared to the AA Model. It could be why free energy in CG-MARTINI Model with electrostatic scale parameter optimized and reached -140.831 kcal/mol and -32.74 kcal/mol in the experiment. Although this makes free energy has no barriers, it cannot describe the binding or unfolded protein process, which is somehow described in free energy analysis in higher electrostatic parameters.

CONCLUSION

Our study concludes that the CG-MARTINI method with windows separation and electrostatic scaling is one alternative method that can reduce the simulation time for the complex system. The free energy values fairly approach the experimental value. The CG-MARTINI describes how it reduces the definition of the atom into beads. CG-MARTINI methods with a MARTINI force field build a protein's structure in an equilibration state. The effects of the addition of lipid membrane, the conformation, and the stabilities have been analyzed from the free energy of the conformation system to find the favorable structure using free energy perturbation (FEP) calculation. FEP calculation results show that a few factors affect free energy values with the CG-MARTINI method: windows separation, electrostatic parameter, and flag characterization parameter.

Interestingly, this work has relationships or scaling between the electrostatic parameter and free energy value. For this reason, we try to rescale for the possibility of running coarse-grained and comparable to all-atom simulation. Our results show that the potential candidate is in tuning the electrostatic parameter, so the electrostatic scaling effect is an interesting parameter.

Our results suggest a kind of scaling to bring CG-MARTINI closer to all-atom by finding a hidden parameter scaling. One of the candidates that we propose is to use electrostatic scaling. With this kind of scale, it is possible to produce free energy values closer to the experimental results. This step could be useful for approaching experimental results. Furthermore, this scale factor can be used by CG-MARTINI for similar cases.

ACKNOWLEDGEMENT

The authors thank the support from the Faculty of Mathematics and Natural Sciences, Institute of Technology Bandung (ITB), Indonesia, through Program Penelitian, Pengabdian Masyarakat, dan Inovasi (PPMI), and partly supported by the Indonesian Endowment Fund for Education (LPDP) Indonesia.

REFERENCES

Adman, E. T., & Jensen, L. H. (1981). Structural features of Azurin at 2.7 angstroms resolution. *Israel Journal of Chemistry, 21*(1), 8-12. https://doi.org/10.1002/ijch.198100003

Arumugam, S., Chwastek, G., & Schwille, P. (2011). Protein–membrane interactions: The virtue of minimal systems in systems biology. *Wiley Interdisciplinary Reviews: Systems Biology and Medicine, 3*(3), 269-280. https://doi.org/10.1002/wsbm.119

Beveridge, D. L., & DiCapua, F. M. (1989). Free energy via molecular simulation: Applications to chemical and biomolecular systems. *Annual Review of Biophysics and Biophysical Chemistry, 18*(1), 431-492. https://doi.org/10.1146/annurev.bb.18.060189.002243

Frauenfelder, H., Chena, G., Berendzena, J., Fenimorea, P. W., Janssonb, H., McMahona, B. H., Stroec, I. R., Swensond, J., & Younge, R. D. (2009). A unified model of protein dynamics. *Proceedings of the National Academy of Sciences, 106*(13), 5129-5134. https://doi.org/10.1073/pnas.0900336106

Gumbart, J., & Roux B. (2012). Determination of membrane-insertion free energies by molecular dynamics simulations. *Biophysical Journal*, *102*(4), 795-801. https://doi.org/10.1016/j.bpj.2012.01.021

Gumbart J., Chipot C., & Schultena K. (2011). Free-energy cost for translocon-assisted insertion of membrane proteins. *Proceedings of the National Academy of Sciences, 108*(9), 3596-3601. https://doi.org/10.1073/pnas.1012758108

Gurtovenko, A. A., & Anwar, J. (2009). Interaction of ethanol with biological membranes: The formation of non- bilayer structures within the membrane interior and their significance. *Journal of Physical Chemistry B, 2009, 113*(7), 1983-1992. https://doi.org/10.1021/jp808041z

Humphrey, W., Dalke, A., & Schulten, K. (1996). VMD-visual molecular dynamics. *Journal of Molecular Graphics, 14*(1), 33-38. https://doi.org/10.1016/0263-7855(96)00018-5.

Jiang, W., Hodoscek, M., & Roux, B. (2009). Computation of absolute hydration and binding free energy with free energy perturbation distributed replica-exchange molecular dynamics (FEP/REMD). *Journal of Chemical Theory and Computation, 5*(10), 2583-2588. https://doi.org/10.1021/ct900223z.

Kucerka, N., Tristram-Nagle, S., & Nagle, J. F. (2006). Structure of fully hydrated fluid phase lipid bilayers with monounsaturated chains. *Journal of Membrane Biology, 208*(3), 193-202. https://doi: 10.1007/s00232-005-7006-8.

Kurniawan, I., Kawaguchi, K., Sugimori, K., Sakurai, T., & Nagao, H. (2019). Theoretical studies on electronic structure and proteins of type I copper center in copper proteins. *Science Report Kanazawa University, 63*, 1-13.

Li, Y., & Nam, K. (2020). Repulsive soft-core potentials for efficient alchemical free energy calculations. *Journal of Chemical Theory and Computation, 16*(8), 4776-4789. https://doi:10.1021/acs.jctc.0c00163.

Marrink, S. J., Risselada, H. J., Yefimov, S., Tieleman, D. P., & De Vries, A. H. (2007). The MARTINI force field: Coarse-grained model for biomolecular simulations. *Journal of Physical Chemistry B, 111*(27), 7812-7824. https://doi.org/10.1021/jp071097f

Mark, A. E. (1998). Free energy perturbation calculations. In P. V. R. Schleyer, N. L. Allinger, T. Clark, J. Gasteiger, P. A. Kollman, H. F. Schaefer & P. R. Schreiner (Eds.), *Encyclopedia of Computational Chemistry* (pp.1070-1083). Wiley and Sons.

Pappalardo, M., Milardi, D., Grasso, D. M., & La Rosa, C. (2003). Free energy perturbation and molecular dynamics calculations of copper binding to Azurin. *Journal of Computational Chemistry*, *24*(6), 779-785. https://doi.org/10.1002/jcc.10213

Phillips, J. C., Hardy, D. J., Maia, J. D. C., Stone, J. E., Ribeiro, J. V., Bernardi, R. C., Buch, R., Fiorin, G., Henin, J., Jiang, W., McGreevy, R., Melo, M. C. R., Radak, B. K., Skeel, R. D., Singharoy, A., Wang, Y., Roux, B., Aksimentiev, A. Luthey-Schulten, Z., … & Tajkhorshid, E. (2020). Scalable molecular dynamics on CPU and GPU architectures with NAMD. *Journal of Chemical Physics, 153*(4), Article 044130. https://doi.org/10.1063/5.0014475

Pohorille, A., Jarzynski, C., & Chipot, C. (2010). Good practices in free-energy calculations. *Journal of Physical Chemistry B, 114*(32), 10235-10253. https://doi.org/10.1021/jp102971x.

Pozdnyakova, I., Guidry, J., & Wittung-Stafshede, P. (2002). Studies of *pseudomonas aeruginosa Azurin* mutants: Cavities in β-barrel do not affect refolding speed. *Biophysical Journal, 82*(5), 2645-2651. https://doi.org/10.1016/S0006-3495(02)75606-3

Pozdnyakova, I., & Wittung-Stafshede, P. (2001). Copper binding before polypeptide folding speeds up the formation of active (holo) Pseudomonas aeruginosa Azurin. *Biochemistry, 40*(45), 13728-13733. https://doi.org/10.1021/bi011591o

Zhu, F., Bourguet, F. A., Bennett, W. F. D., Lau, E. Y., Arrildt, K. T., Segelke, B. W., Zemla, A. T., Desautels, T. A., & Faissol, D. M. (2022). Large-scale application of free energy perturbation calculations for antibody design. *Scientific Reports*, *12*, Article 12489, https://doi.org/10.1038/s41598-022-14443-z